

Shailesh Kumar Shinde¹,
 Dr. Santosh Pawar^{1*}
 Dr. Om Prakash
 Choudhary²

Design and Comparative Analysis between Waveguide Directional Coupler and Multi-mode Interference Coupler for Optical Communication System



Abstract: Recently integrated optical fiber based components plays a important role as optical-MEMS in the optical communication system. In this paper, we optimized design and simulated various kinds of 3dB integrated waveguide beam splitter such as directional coupler (DC), multimode interference (MMI) coupler. These all components optimized for suitable waveguide material such as polymer, Lithium Niobate, silicon etc. Optical directional coupler and multimode interference coupler have been designed, optimized and simulated for optical communication system (OCS).

Keywords: optical MEMS, integrated optics, DC, MMI, optical communication, silicon, Lithium Niobate, SU8 polymer.

1. INTRODUCTION

Optical waveguides are the fundamental components of integrated optical circuits (IOCs) for the optical communication system which connect all optical active and passive elements to relay all optical signal processes such as splitting, filters, modulating, amplifying and detecting. Integrated optical waveguide is same as electronic integrated circuits (ICs) wherein the light is confined in the waveguide along the direction of waveguide instead of the electron in the electronic circuit [Hunsperger, 1991]. There are several ways to categorize optical waveguides, including by their geometry (planar, channel, rib/ridge waveguides), mode structure (single-mode, multi-mode), refractive index distribution (step or gradient index), and material (glass, polymer, semiconductor). Figure1 depicted the commonly used optical waveguide geometries in integrated optics. Integrated optical waveguides have a high-index core that is surrounded by a low-index cladding as an optical fibre. The refractive index contrast between the core and the cladding is much higher for silicon on insulator (SOI) waveguides as well as Lithium niobate and high index polymers.

Although, the optical mode is much tightly confined in to the core, allowing less than a micron size waveguides and very small bend radii. Waveguide can have a $5\mu m$ bend radius, losing only 0.01dB power per 90° bend. However, the small waveguide size has also its disadvantages: high propagation loss and sensitive to fabrication tolerances. The propagation loss in waveguides is caused mainly by the scattering at the sidewalls of the waveguide [Yapet al., 2009]. The reason for the scattering is the roughness created during the etching process. By using shallow-etched rib waveguides, the overlap between the E-field and the sidewalls of the waveguide can be reduced. Propagation loss of 0.27 dB/cm for 470 nm wide, shallow-etched rib waveguides have been demonstrated [Bogaerts, 2011]. The confinement of the fundamental mode in a shallow-etched rib waveguide is not as tight as the confinement in a ridge waveguide. In recent years, optical parts are usually built by introducing modifications to the waveguide structure such as changing the geometry and altering or actively manipulating the physical properties of the waveguide. Devices such as splitters, filters, modulators, amplifiers, lasers and detectors have been demonstrated in different materials systems [Kaminow, 2008].

¹Department of Electronics & Communication,
 Dr. A. P. J. Abdul Kalam University, Indore (M.P.), India - 452016

²Department of Physics, Dr. A. P. J. Abdul Kalam University, Indore (M.P.), India - 452016

*Corresponding author Email: spawarrkdf@gmail.com

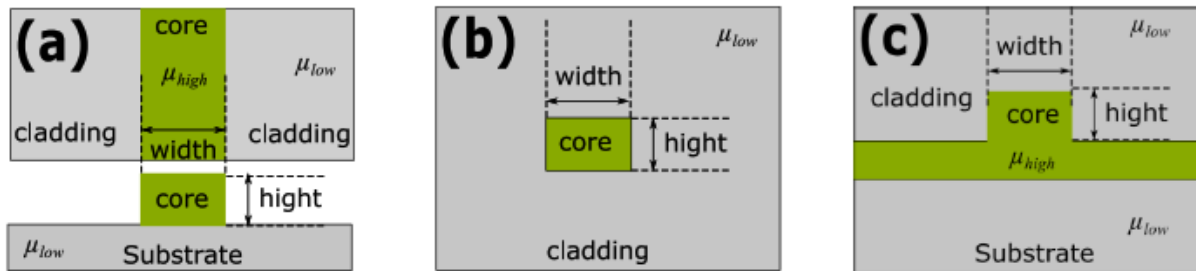


Figure 1: Optical Waveguides can be classified according to their geometry. (a) slab or planar waveguide, (b) buried waveguide, (c) ridge/rib waveguide.

A broad review on active component is presented [Park et al., 2011]. In addition to active components, electronic and photonic integration can be combined on the same material system, which can further miniaturize electro-optical systems [Orcutt et al., 2012]. Optical coupler is a basic part for the optical device and application [Tsao and Chu-yi, 2002], which can be used as beam splitter/beam combiner within optical communication system. There are several types of integrated optical couplers for 3dB coupling function such as Y-junction [Zhang et al., 2013], Directional coupler [Yamada et al., 2005], Multimode interference [Sheng et al., 2012], Single mode or two mode interference couplers. As exhibited in Figure 2, the directional coupler can be used as a beam splitter/combiner in an on-chip Michelson interferometer. It can be fabricated in different materials such as semiconductor, silicon on insulator, Lithium Niobate and polymer etc. Y-junction splitters have the most compact size and polarization insensitive behaviour in single mode interference coupler, but their sharp edges on Y-junction is unpractical for fabrication due to the limited resolution of etching process. But many issues arise in directional coupler (DC) about fabrication tolerance, wavelength sensitive etc.

DC is wavelength sensitive and the material used for fabrication the waveguide may have birefringence due to the long waveguide and non-trivial waveguide geometry. It is discussed on the crosstalk, polarization and birefringence properties of the directional couplers [Chen et al., 2013]. Also, the splitting ratio of DC are not constant (differs from 3dB) over a broad spectral range. Wavelength-insensitive couplers such as MMI couplers could solve this problem by providing an almost constant splitting ratio over broad spectral ranges (≥ 100 nm) without introducing any excess loss. Single-mode interference (SMI) couplers are essentially lossy as two modes are inevitably excited at the Y-junction, with equal intensities, of which one cannot be guided and is thus lost as radiation. Two-mode interference (TMI) couplers are also lossy due to the required sharp features that cannot be faithfully reproduced by current lithographic techniques. Multimode interference (MMI) based devices have proceeded rapidly due to their attractive properties such as compactness [Stevanus and Chee-Wei, 2005], tolerance to a range of fabrication parameters, an inherent balance, polarization insensitive and low optical loss and because they are particularly well suited to use with a moderate number of ports. Detail structure of MMI is shown in sets as shown in Figure 2. Waveguide coupler may have different structural design as per requirement for single mode or multimode coupler. The channel waveguide at the interaction region could be just sandwiched 100% or 50% as may be requirement.

DC are fabricated by arranging two channel waveguides with appropriate lateral gap. The coupling (interaction) length depends on the gap between two waveguides. The gap may be of several microns long because the coupling lengths of their coupled waveguides range from several hundred micrometres. Furthermore, to transfer optical power to and from two waveguide cores separately, we need four sets of S-shaped waveguides of several microns long for the input and output ports. Since these waveguides cannot be bent to a radius of less than few λ .

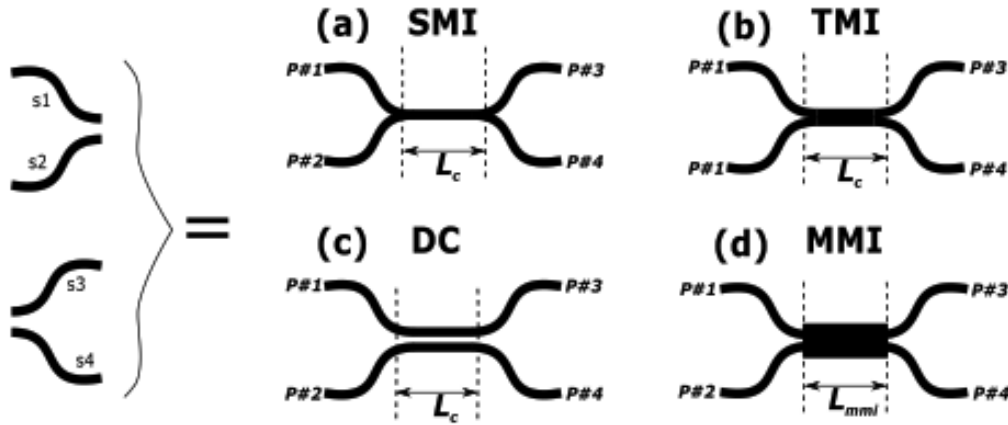


Figure 2 : Construction of integrated optical couplers using four ‘S’ shaped Waveguides. (a) Single mode interferometer (SMI), (b)Two mode interferometer (TMI), (c) Directional coupler (DC), (d) Multimode interferometer (MMI). Wherein L_c is coupling length for DC, L_{mmi} is the coupling length for MMI coupler and $P_{\#1}, P_{\#2}, P_{\#3}, P_{\#4}$ are all the access input/output ports.

2. DESIGN AND SIMULATION OF DIFFERENT WAVEGUIDE GEOMETRY

Waveguide geometry is an important part of the optical system that connects all optical components of the system. Optical system consists of multitudes of optical waveguides which should have good transmission characteristics for the wavelength range associated with the broadband source. They have to be single mode and the overall propagation losses and birefringence have to be low. The index contrast $(\mu_{high} - \mu_{low}) / \mu_{high}$ and the waveguide geometry determine the divergence of the free-space beam emerging from sample and reference arms. For the optical applications, the waveguides should be designed to produce a low-divergence output beam with concentration $\cong 1$ while maintaining a small device size.

A deep etched ridge waveguide geometry is chosen as the basic building block of all integrated optical devices in this section due to its smaller bending radius and high fabrication tolerance compare to another waveguide counterpart. There are three design parameters for a channel waveguide; waveguide width (W), height (H), and index contrast (index difference between core (μ_{high}) and cladding (μ_{low}) layers as depicted in Figure 3 (a) and (b). Depending upon the operation wavelength range of the optical communication system (OCS) applications (around 850nm, 1330nm and 1550nm), different waveguide geometries were designed for these ranges. Besides single-mode, low loss (0.1 dB/cm), and waveguide birefringence, which is designed as the difference between the effective index for the transverse-magnetic (TM) and transverse-electric (TE) polarizations, operation of these waveguides, their lateral and vertical beam divergence should be low (and preferably close to each other) in order to reduce chip-to-sample coupling losses. Designing parameter of the waveguide initially selected as; $W=2 \mu m, H=1.5 \mu m$. PMMA/SU-8 were selected as waveguide material with $\mu_{high}=1.57$ and $\mu_{low}=1$.

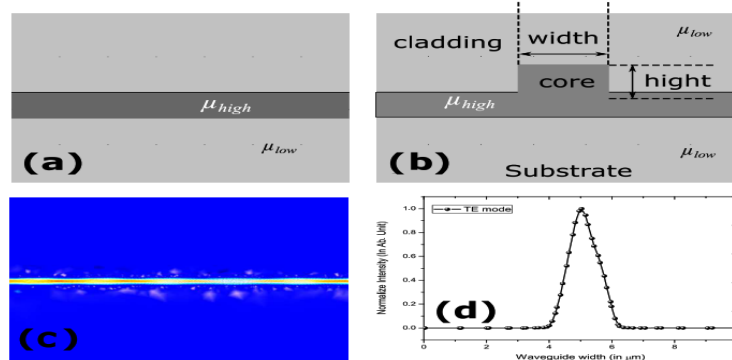


Figure 3: Waveguide geometry simulation as: (a) Top view, (b) cross section, (c) propagation field along the waveguide and (d) Normalize power along the waveguide without any losses.

The simulations were performed using *COMSOL Multiphysics* [COMSOL, 2015] and *RSoftBeamProp* [BeamPro, 2014] software. Initial simulation was performed with simple linear waveguide shown in Figure 3. It is clearly seen propagating *TE* field along the waveguide with low optical loss in Figure 3 (c) and normalized power graph Figure 3 (d). Other waveguide geometries have been also simulated are shown in Figure 4 (a) Simulated structure waveguide, (b) Simulation of the S-bend with design radii, (c) C-bend channel, and (d) Mirror loop waveguide simulation for the back reflection of the wave as a mirror without loss [Jun-long et al., 2012]. The effective refractive index, minimum bending radius, coupling and bending losses, and the minimum acceptable gap between waveguides were extracted from simulation results.

3. OPTICAL WAVEGUIDE DIRECTIONAL COUPLER

A crucial part for numerous integrated optical functional devices, optical directional couplers (DC) are found in power splitting and combiner, add drop multiplexing [Ofusa et al., 1999], switch [Kogelnik and Schmidt, 1976], and signal modulation. In particular, optical waveguide based on semiconductor, lithium Niobate, silicon and high index polymer material system have attracted considerable attention because of their ultra-small size, strong confinement of light, low losses and small radii. These materials are an ideal choice for monolithic or heterogeneous (hybrid) fabrication technology since they can support both active and passive optical functions including laser, modulator, detector and all type of integrated optical parts.

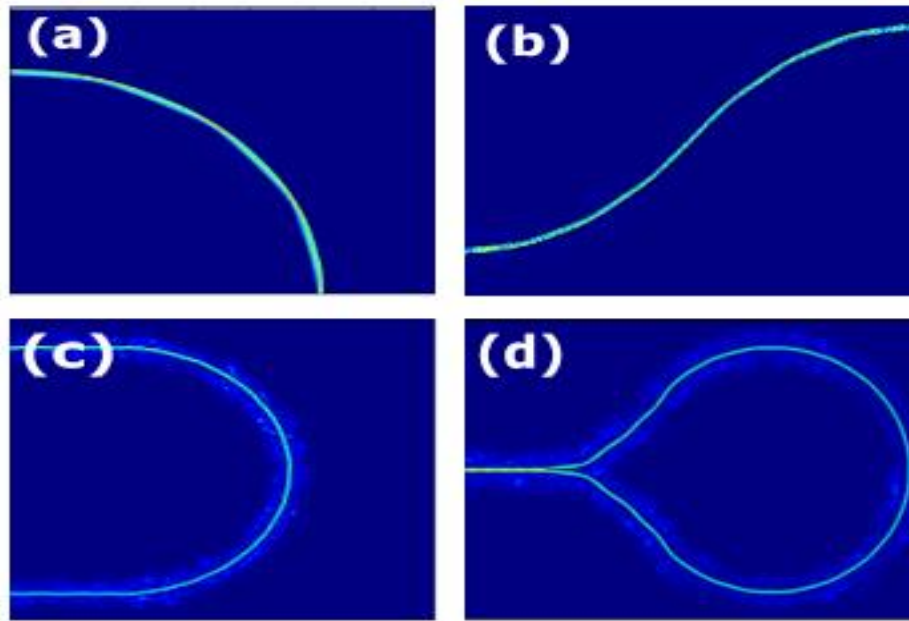


Figure 4: Different waveguide geometry simulation done for (a) L-bend structure waveguide, (b) S-bend with designed radii of curvature, (c) C-bend and (d) Mirror loop waveguide.

Optical waveguide directional coupler consists of two parallel waveguides placed at separate

of small gap (g_{DC}) shown in Figure 5 with connecting S-bend waveguide for input/output access port. Due to FTIR, optical power can be travel from one waveguide to adjacent waveguide as a result of the overlap in the evanescent fields of the two waveguides. The amount of power transferred between the waveguides depends upon the waveguide parameters, i.e., the guided wavelength, the confinement of the individual waveguides, the separation between them, the length over which they interact, and the phase mismatch between the individual waveguides [Ternoven et al., 1993].

According to the coupled mode theory (CMT), coupling coefficient κ between the two optical modes propagating in the optical waveguides that form a symmetric directional coupler can be expressed as, [Lui, 2005]

$$\kappa = \frac{1}{2}(\beta_e - \beta_o) \quad (3.1)$$

Where β_e and β_o are the propagation constants of the even and odd super-modes. The coupling length L_c of a directional coupler may be defined as related to the coupling coefficient κ by

$$L_c = \frac{\pi}{2\kappa} \tag{3.2}$$

$$L_c = \frac{\pi}{(\beta_e - \beta_o)} \tag{3.3}$$

By neglecting the losses, and when the two super-modes are out of phase, the light is completely transferred to the adjacent waveguide. The transfer occurs continuously and periodically as a function of propagation distances z . In the ideal symmetric case, the output powers in the bar and cross waveguides are given by

$$P_{\#3} = P_{\#1} \cos^2\left(\frac{\pi z}{2L_c}\right) \tag{3.4}$$

Where $P_{\#1}$ is the input power and L_c is the coupling length.

$$P_{\#3} = P_{\#1} \sin^2\left(\frac{\pi z}{2L_c}\right) \tag{3.5}$$

Where $P_{\#3}$ and $P_{\#4}$ are the splitted output powers of power $P_{\#1}$.

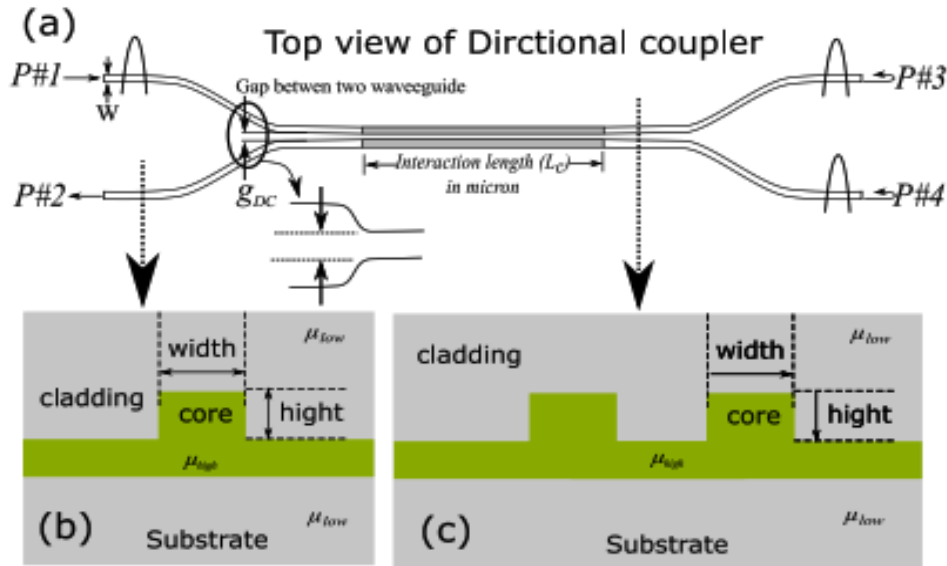


Figure 5: (a) Schematic of the symmetric directional coupler design, (b) and (c) cross sectional view

4. DIRECTIONAL COUPLER DESIGN AND SIMULATION

Geometrical dimension of optical directional coupler is considered according to Figure 5, while the cross section for each of ridge waveguide and the light coupling amount of power transferred between the waveguides depends upon the waveguide parameters, i.e, the guided wavelength λ_c , waveguide width W , waveguide height H , the separation between them g_{DC} and the waveguide material index refraction. These are all waveguide polarization insensitive, birefringence etc.

In this section, we study and simulate directional coupler based on Silicon/Polysilicon, Lithium Niobate, and Polymer (PMMA and SU-8) for comparative study to realize a smallest directional coupler as well as low loss, polarization independent etc. Optical directional couplers in these three material waveguides have been investigated by using a semi-analytic approach based on both Finite Element Method (*FEM with COMSOL MultiPhysics* Software) and Beam Propagation Method (*BMP with R-Soft*). To validate this approach with the simulation Software, we have simulated the proposed in Reference [Yamada et al., 2005]. In which, the dependence of the normalized optical power at the parallel (bar) and cross ports as a function of coupling length L_c are demonstrated in Figure 6. The simulated result indicates a coupling length L_c of $9.8\mu m$ and $11.2\mu m$ for *quasi-TM* and *quasi-TE* modes, respectively, these results are in good agreement with those reported in

reference [Yamada et al., 2005] $L_c=10\mu m$ for *quasi-TM* and $L_c=11\mu m$ for *quasi-TE* mode, obtained experimentally and theoretically by 3D Finite-Difference Time Domain (FDTD) approach.

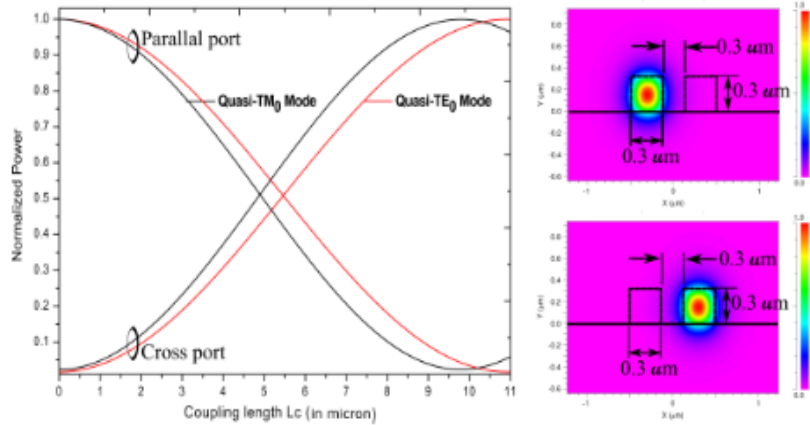


Figure 6: Dependence of the normalized optical power at the parallel (bar) and cross ports as a function of coupling length L_c for this device in [Yamada et al. 2005]

For qualitative design and comparative analysis of directional coupler, we considered waveguide core material as silicon (Si), Lithium Niobate (LN) and Polymer (SU-8 or PMMA). We focused mainly on characteristic of 3dB Directional coupler. Dependency of the 3dB coupling length on spectral range (wavelength), waveguide width, separating gap between the waveguide and as well as power splitting ration with coupling length for all these materials are simulated. We also compared results for best waveguide or active/passive waveguide component among of these to fabricate optical communication system.

DC characteristic is simulated using 2D beam propagation method (*RSoftBeamPROP*) as a function of wavelength with 3dB coupling length for various waveguide width and also characterized 3dB coupling length for different waveguide width, 3dB coupling length characteristics as function of gap between two parallel waveguides have been demonstrated for different material and analysed them. In the following section, we are using the design of Si, LN and SU-8/PMMA as waveguide material.

Silicon (Si):

Silicon technology has eminence possibility towards fabrication of highly dense optical component on single Silicon on Insulator platform for various application and signal Processing [Reed and Knights, 2005]. Si based materials are ideal choice for monolithic integration, since they can support both active and passive optical functions, including, lasers source, detectors and passive waveguides. Silicon ridge waveguide are the attractive structure to use for optical interconnections as well as DC on SOI chip. Waveguide bending radius can be less than a few microns due to high refractive index of Si core (core=3.5) silica cladding (clad=1.5).

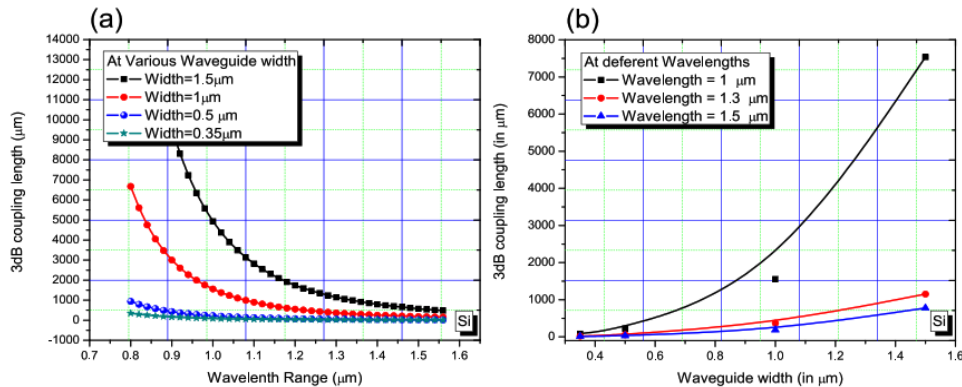


Figure 7 : Directional coupler characteristics of silicon as: (a) Coupling length dependence on wavelength for different width of waveguide, and (b) Coupling length vs widths of waveguide for different wavelength.

Silicon DC characteristic has been simulated using 2D beam propagation method (*RSoftBeamPROP*) as a function of wavelength with 3dB coupling length for various waveguide width are exhibited in Figure 7. In general observation, Figure 7(a) shows the wavelength increases at waveguide width ($W=2\mu\text{m}$) and different gap between two adjacent waveguide of DC than the coupling length exponentially decreases, while Figure 7(b) shows the width increase at fixed gap ($g_{DC}=0.2\mu\text{m}$) and different wavelength than 3dB coupling length increases. It means, 3dB coupling length of Si directional coupler is strongly dependent on the guiding wavelength as well as waveguide width. 3dB coupling length (L_c) has dependency on gap (g_{DC}) as in Figure 8 for different wavelength. Figure 8 (a, b, c) shows, the 3dB coupling length (L) increases on increasing the gap (g_{DC}) for TE_0 and TM_0 modes.

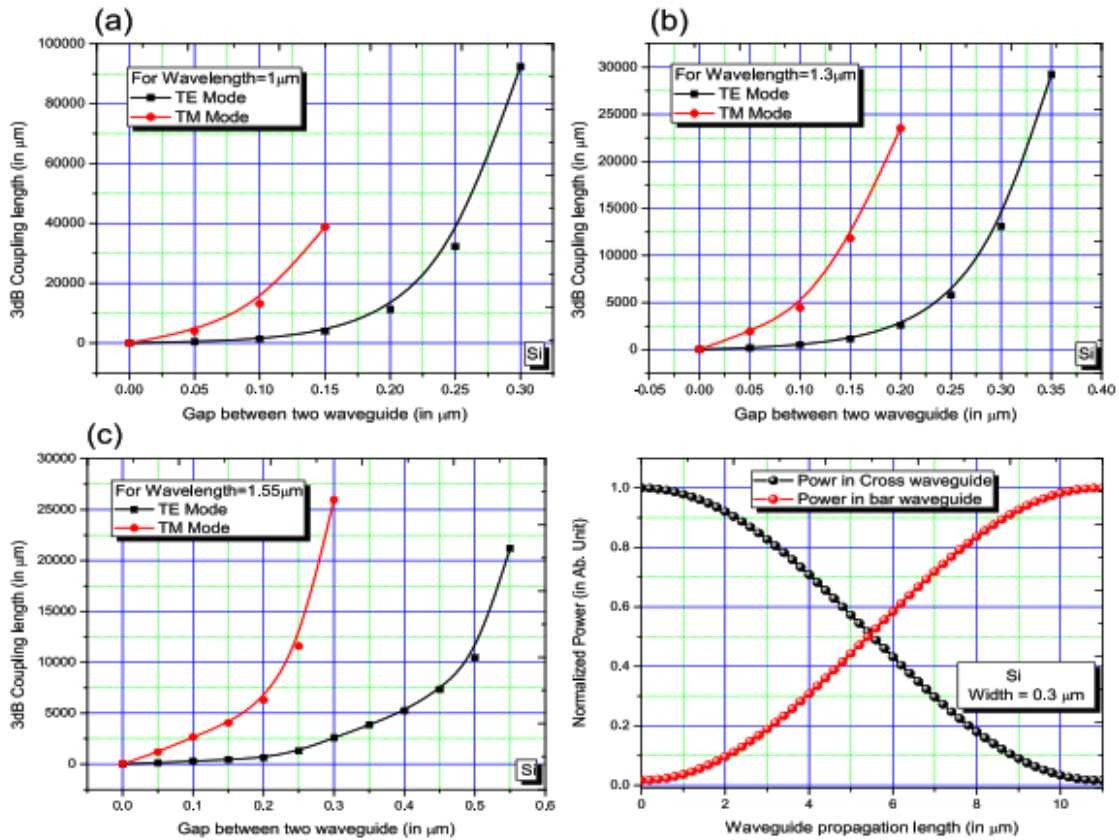


Figure 8: Directional coupler characteristics of silicon as wavelength material with fixed width of waveguide as: (a) Coupling vs gap between waveguides for $\lambda=850\text{ nm}$, (b) $\lambda=1.33\mu\text{m}$ and (c) $\lambda=1.55\mu\text{m}$ and (d) normalized power Vs waveguide propagation length.

Lithium Niobate (LN):

Lithium Niobate (LN) is promising material for integrated optical circuits. Due to their excellent electro-optic, thermo-optic, acousto-optic, piezoelectric and nonlinear-optic coefficient. LN waveguide can be fabricated generally with two kinds of the method [Il'ichevet al., 2009; Hongsik, 2016]. The first method is, Titan in diffusion, leads to an increase in both the ordinary and extraordinary refractive indices in this birefringent crystal. The second method is proton exchange processes, where the extraordinary refractive index alone increases.

Lithium Niobate directional coupler characteristic as been simulated and exhibited as a function of wavelength with 3dB coupling length for various waveguide width and also characterized 3dB coupling length for different waveguide width depicts in Figure 9. It shows that the coupling length exponentially decreases with increase in, while Figure 9(b) shows that the 3dB coupling length increases for increase on waveguide width for all wavelength. It means, 3dB coupling length of LN Waveguide directional coupler is strongly dependent on the guiding wavelength as well as on the waveguide width. The 3dB coupling length (L_c) dependence on gap (g_{DC})

as depicts in Figure 10. It is observed in Figure 10 (a,b, c) that, the 3dB coupling length (L_c) increases on increasing the gap for TE_0 and TM_0 modes.

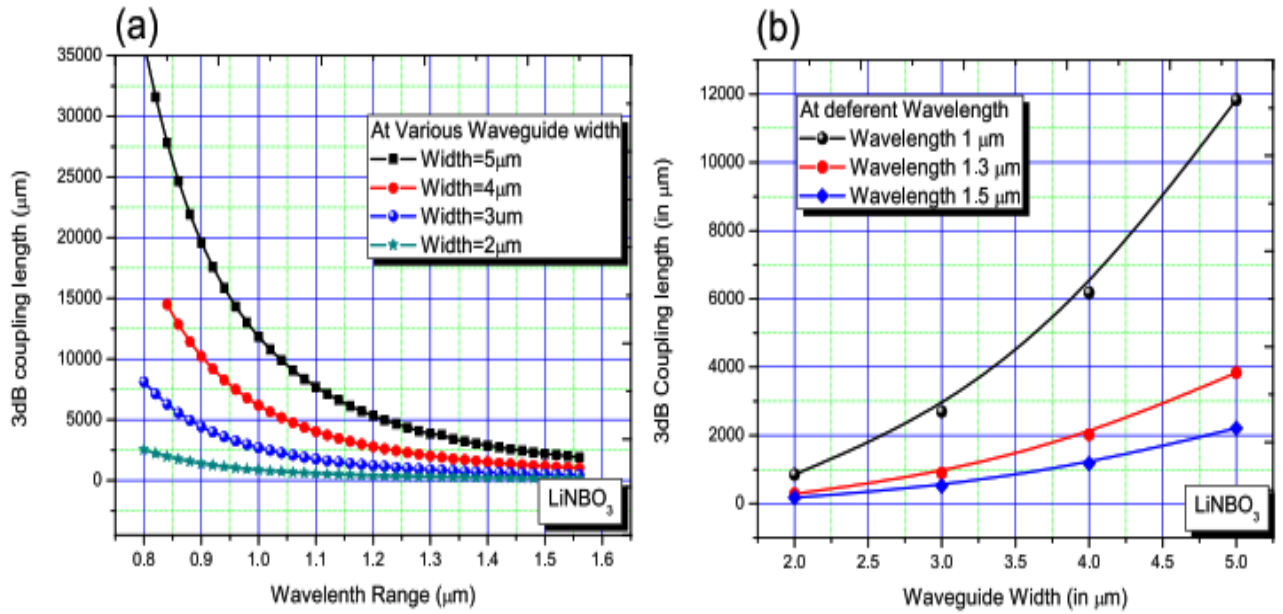


Figure 9: Directional coupler characteristic of Lithium Niobate as: (a) Coupling length Vs wavelength range with different waveguide width (b) Coupling length Vs Waveguide width with different wavelength.

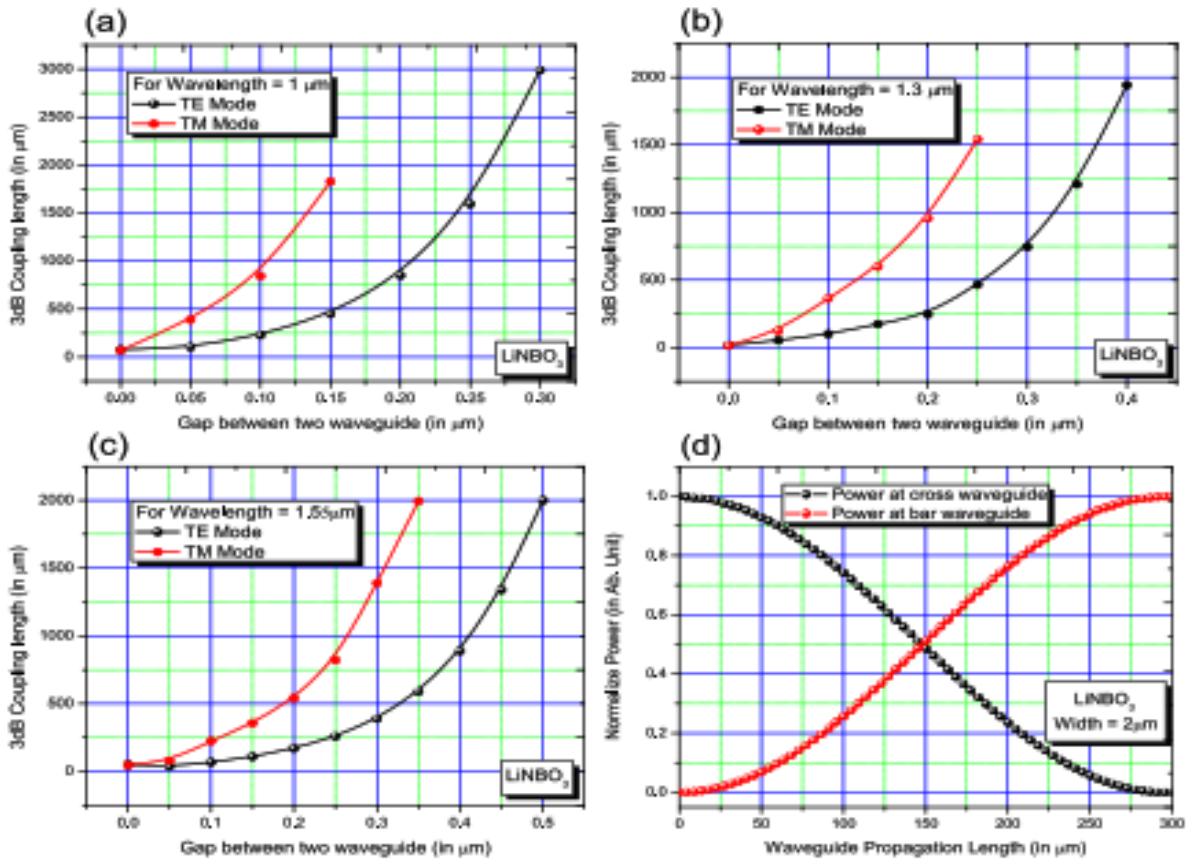


Figure 10: 3dB directional coupler characteristics of Lithium Niobate with fixed width of waveguide as: (a) 3dB coupling Vs gap between waveguide for wavelength=1 μm , (b) 3dB coupling Vs gap between waveguide for wavelength=1.3 μm , (c) 3dB coupling Vs gap between waveguide for wavelength=1.5 μm , and (d) Ration of normalized power varies with varying waveguide propagation length.

Polymer waveguide using SU-8/PMMA:

SU-8 polymer is highly demanded material towards hybrid fabrication for integrated optics or optical MEMS [Wayant, 2000, Chollet, 2009] because of it has unique physical, chemical, mechanical, electromagnetic and biocompatible properties amongst all other optical material. Moreover, combination of SU-8 based integrated optics with microelectronics allow the development of complex MOEMS for sensing application. currently, SU-8 is most preferred material for fabrication of optical waveguide, grating, reflector, Photonic band gap structure, on chip light source, optical pressure sensor, opto-fluidic system [Nordstrom et al., 2007; Gharari et al., 2008; Xie et al., 2008] due to, high transparency above 400 nm, waveguide circuit can be easily fabricated using simple techniques for mass fabrication such as photolithography and molding.

SU-8 polymer DC characteristic has been simulated and characterized as a function of wavelength with 3dB coupling length for various waveguide width and also characterized as function of waveguide width with 3dB coupling length for different wavelength shown in Figure 11. In general observation, Figure 11(a) shows the wavelength increases at width ($W=2\mu\text{m}$) and various gap than the coupling length exponentially decreases, while Figure 11(b) shows the width increase at fixed gap ($g_{DC}=0.2\mu\text{m}$) and different wavelength than 3dB coupling length increases. It means, 3dB coupling length of Si directional coupler is strongly dependent on the guiding wavelength as well as waveguide width. The 3dB coupling length (L_c) also dependent on gap (g_{DC}) depicted in Figure 12 for TE_0 and TM_0 modes. It observed From Figure 12 (a, b, c), the 3dB coupling length (L_c) increases on increasing the gap (g_{DC}).

In further investigation, design and material parameters are listed in Table 1 for direction coupler. The simulation results for the designed directional coupler's coupling length are displayed in Table 2. The resultant 3dB coupling length for Silicon, Lithium Niobate and SU-8 Polymer is $L_c=186\mu\text{m}$, $L_c=169.5\mu\text{m}$, $L_c=47\mu\text{m}$ for TE Mode and $L_c= 635\mu\text{m}$, $L_c=535.5\mu\text{m}$, $L_c=65\mu\text{m}$ for TM mode respectively.

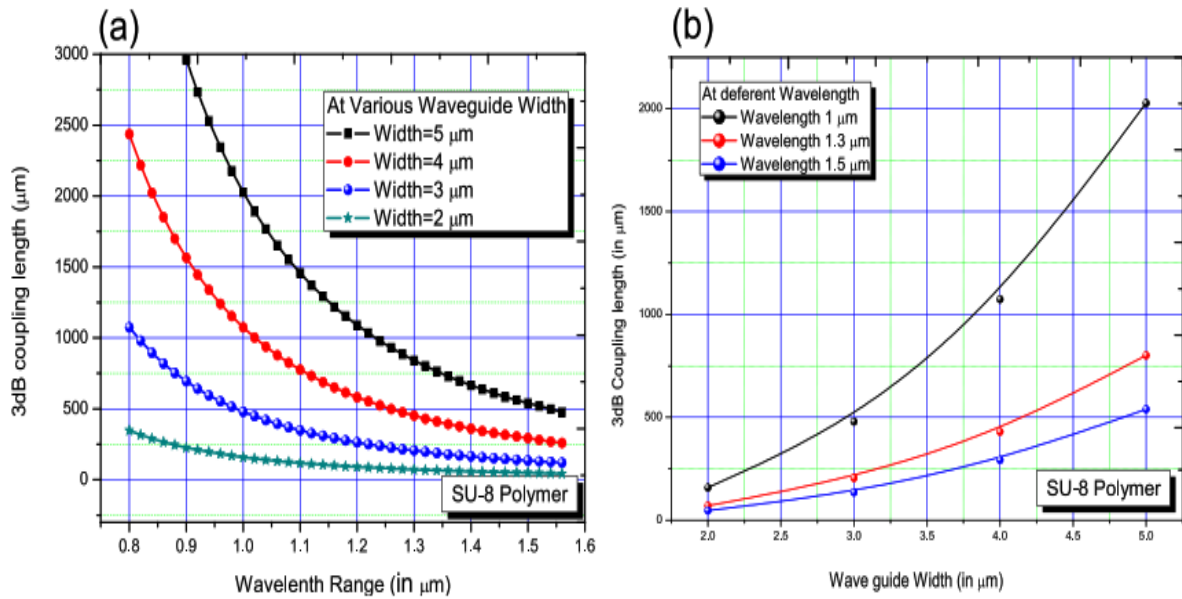


Figure 11: Directional coupler characteristic of SU-8 Polymer as: (a) Coupling length Vs Wavelength rang with different width, (b) Coupling length Vs Waveguide width with different wavelength.

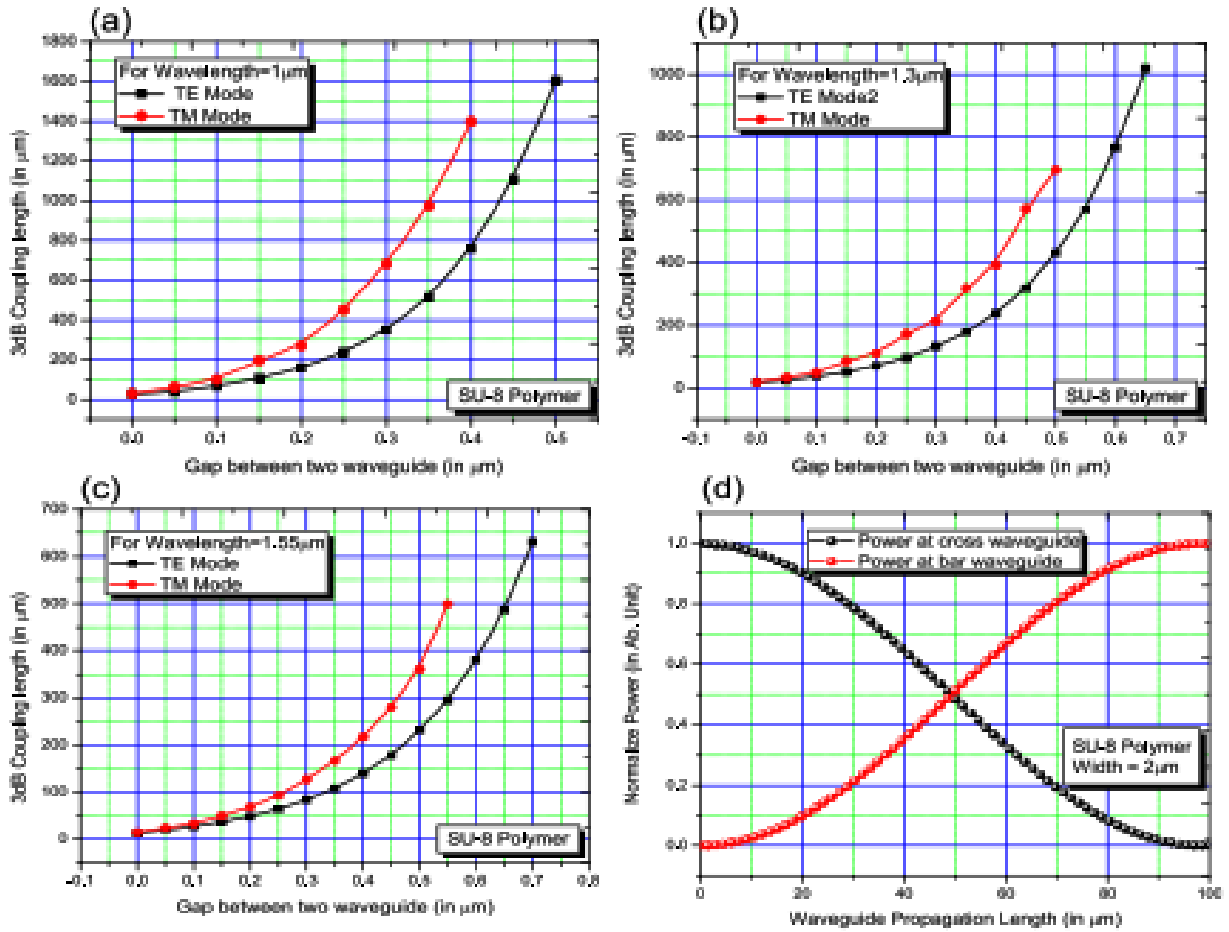


Figure 12: Directional coupler characteristic of SU-8 polymer with fixed width of waveguide as; (a) Coupling Vs gap between waveguide for $\lambda_c = 1\mu\text{m}$, (b) $\lambda_c = 1.3\mu\text{m}$, (c) $\lambda_c = 1.5\mu\text{m}$, and (d) normalized Power Vs waveguide propagation length.

Table 1: Design of DC coupler with structural parameter for different materials.

S. No.	MMI design parameters with different materials	W (in μm)	(g_{DC}) (in μm)	μ_{core} (in μm)
1	Design 1 DC(Si)	2	0.2	3.5
2	Design 1 DC(LN)	2	0.2	2.5
3	Design 1 DC(Su-8)	2	0.2	1.5

Table 2: Results of DC coupler for different structural and material parameters.

S. No.	MMI Design with different materials	λ_c (in μm)	L_c for TM_0 (in μm)	L_c for TE_0 (in μm)
1	Design 1 DC (Si)	1.55	635	486
2	Design 1 DC (LN)	1.55	535.5	169.5
3	Design 1 DC (Su-8)	1.55	65	47.5

5. MULTIMODE WAVEGUIDE COUPLER

Compared to other waveguide coupling structures like directional couplers, MMIs offer a number of benefits, such as reduced size, a wider operating bandwidth, and a lenient fabrication tolerance. The MMI coupler consist of a lateral Multimode waveguide as shown in Figure 13 where the interference between the modes leads to well defined images of the exciting field at specific imaging lengths within the MMI section. Since the quadrature relationship of the propagation constants for the higher order modes is approximately holds, at one beat length L , most of the input power appears in the output port and produces a mirror-image of the input. At twice the beat length, the power at the output end, P#3 and P#4 are denied as those ports which are directly opposite the input port in and at equal distance from the symmetry plane respectively. The MMI is based on the self-imaging principle arising from multimode interference [Soldano and Penning, 1995]. For a multimode waveguide supporting m lateral modes, the output field at a distance $z=L$ is given in the 2-D approximation by;

$$\psi(y, L) = \sum_{m=0}^{m-1} C_m \varphi_m(y) \exp\left(i \frac{m(m+2)\pi}{3L\pi} L\right) \tag{3.6}$$

Where C_m is the excitation coefficient for mode m , φ_m is the m the eigen mode and $L_{\pi} = \pi / (\beta_o - \beta_e)$ is the beat length between the fundamental and first-order modes defined as;

$$L_{\pi} = \pi / (\beta_o - \beta_e) = \frac{4}{3} \mu_{eff} (W_{eq}) / \lambda_c \tag{3.7}$$

Where β_o and β_e are propagation constants of the first and the second modes in the MMI section, μ_{eff} is the effective index, λ_c is the operating wavelength, and W_{eq}^2 is the equivalent MMI width as W_{mmi} , which for present case is essentially the same as the physical width of the ridge slab waveguide. There are two basic self-imaging interference along the MMI section for optical coupler and multimode resonances can be achieved either at MMI section lengths which are multiple of $3L$ (general multimode resonances), or MMI section lengths which are multiple of L (restricted multimode resonances). The advantage of using ridge waveguide, as compared to rib waveguide, L will be smaller, since W_{eq} is smaller for the same MMI width, and given number of modes in the MMI can be obtained using a much smaller width, Hence, MMI based on ridge waveguide will. In this simulation study, “restricted resonance” MMI couplers are used. In the restricted interference devices, input/output access waveguides are placed at points $W_{mmi}/4$ from the center of MMI width (W_{mmi}) to avoid crosstalk and scattering loss.

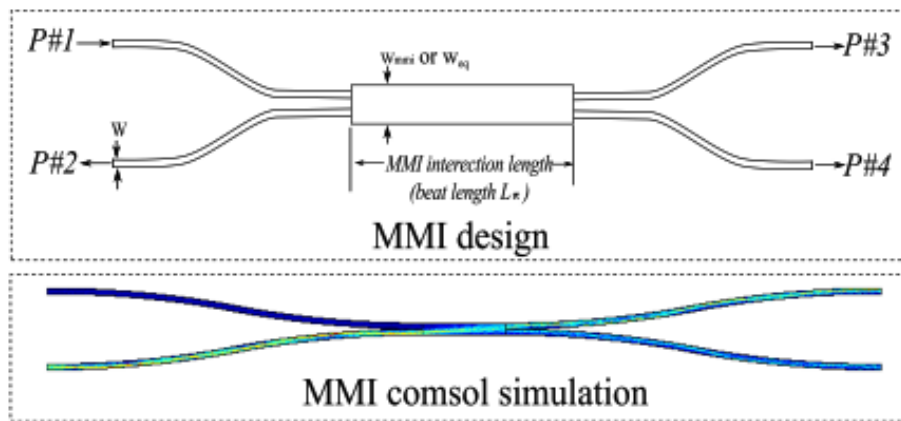


Figure 13 : Schematic sketch of the MMI four port coupler, where as L_{π} is beat length.

MMI Design & Simulation

For design, simulation and comparative analysis of MMI couple based on various waveguide material such as silicon (Si), Lithium Niobate (LN) and Polymer (SU-8 or PMMA). We focused mainly on characteristic of 3dB MMI coupler as, dependency of the 3dB coupling length on the operating wavelength, waveguide width (W_{eq}) or (W_{mmi}) as well as power splitting ration with coupling length. MMI characteristic has been simulated using 2D beam propagation method (*RSoftBeamPROP*). Designed MMI coupler's parameter for simulation of all these materials shown in Table 3 MMI section Waveguide width has been considered as $W_{mmi} = 3W$, where W is the

input access waveguide width. Simulation performed with material as Silicon, Lithium Niobate and SU-8 Polymer. Input/output of the access waveguide absorption/scattering is completely neglect in simulation.

Table3: Design of MMI coupler with parameter for different materials.

S. No.	MMI design parameters with different materials	W (in μm)	W_{mmi} (in μm)	μ_{core} (in μm)
1	Design 1 MMI(Si)	2	6	3.5
2	Design 1 MMI(LN)	2	6	2.5
3	Design 1 MMI(Su-8)	2	6	1.5

Figures 3.14 to 3.16 demonstrates results for designed materials. These all Figures depicts characteristics of the 3dB MMI coupler for particular design consideration as (i) 3dB coupling length is function of coupling wavelength at various width (W) for TE mode only, where it is observed that, if increase wavelength, then 3dB coupling length will be decreases exponentially. (ii) 3dB coupling length also dependent on waveguide width or MMI width for TE or TM modes and realized that, if the width increases then 3dB coupling length will be increases.

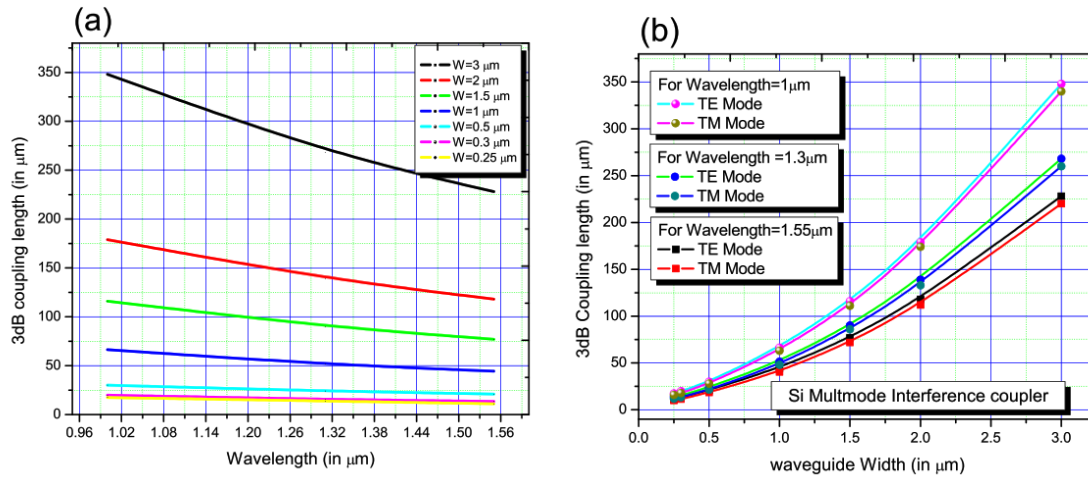


Figure 14: Silicon based MMI coupler characteristic as: (a)Coupling length depend on different wavelength, (b) Coupling length depend on varying waveguide width.

As the resultant 3dB coupling length for Silicon, Lithium Niobate and SU-8 Polymer is $L=118\ \mu\text{m}$, $L=115\ \mu\text{m}$, $L=74\ \mu\text{m}$ for TE Mode and $L=122\ \mu\text{m}$, $L=110\ \mu\text{m}$, $L=71\ \mu\text{m}$ for TM mode respectively shown in the Table 4.

Table 4: Simulation results for designed MMI coupler for $\lambda_c = 1.55$

S. No.	MMI Design with deferent materials	λ_c (in μm)	L_{π} for TM_0 (in μm)	L_{π} for TE_0 (in μm)
1	Design 1 MMI(Si)	1.55	122	118
2	Design 1 MMI(LN)	1.55	115	110
3	Design 1 MMI(Su-8)	1.55	74	71

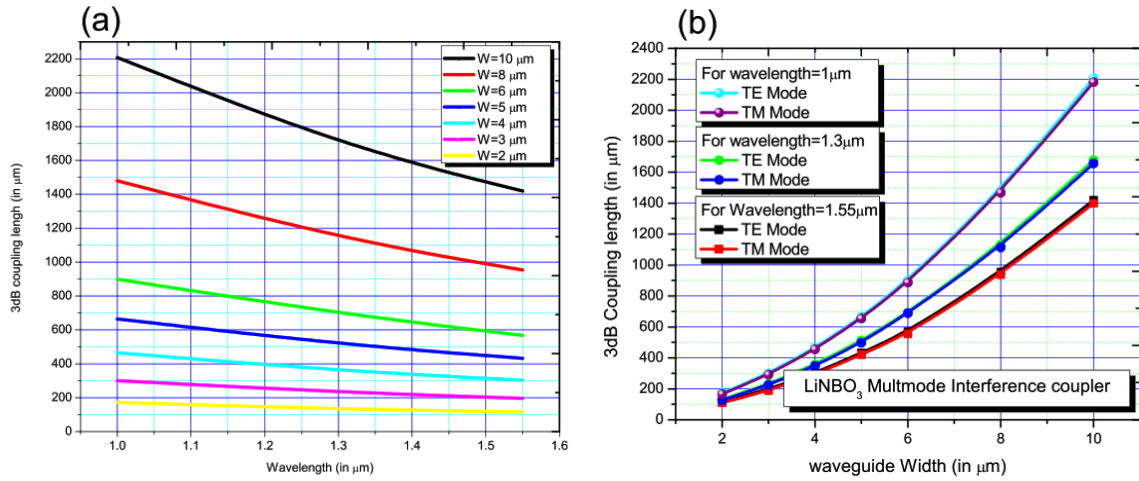


Figure 15 Lithium Niobate based MMI coupler characteristic as: (a) Coupling length depend on different wavelength, (b) Coupling length depend on varying waveguide width.

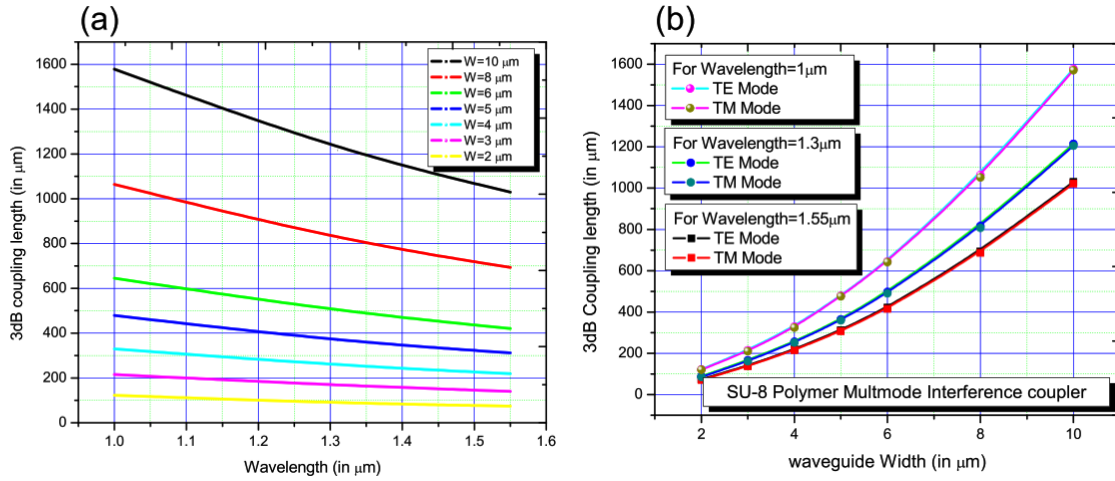


Figure 16: SU-8 based MMI coupler characteristic as: (a) Coupling length depend on different wavelength, (b) Coupling length depend on varying waveguide width.

6. RESULT AND CONCLUSION

Two types of optical coupler designed, simulated and analysed based on different optical material as (i) Directional coupler (ii) multimode interference. Directional coupler characteristic has been simulated and characterized as a function of wavelength with 3dB coupling length for various waveguide width and also characterized as function of waveguide width with 3dB coupling length for different wavelength shown in Figure 7 to 3.11. In general observation, if the wavelength increases at width ($W=2\mu m$), then the coupling length exponentially decreases. And if the width and gap increases with different wavelength, than 3dB coupling length increases. It means, 3dB coupling length directional coupler is strongly dependent on the guiding wavelength as well as waveguide width and it also dependent on gap (g_{DC}). As simulating material and structural design parameter shown in table 3.2, The resultant 3dB coupling length for Silicon, Lithium Niobate and SU-8 Polymer is $L_{\pi}=118\mu m$, $L_{\pi}=11\mu m$, $L_{\pi}=74\mu m$ for TE Mode and $L_{\pi}=122\mu m$, $L_{\pi}=110\mu m$, $L_{\pi}= 71\mu m$ for TM mode respectively.

Characteristics of 3dB MMI coupler based on different material such as Silicon, Lithium Niobate and SU-8 Polymer shown in Figure 3.14 to 3.16 respectively. These all graphs depict, at the higher wavelength for particular wavelength range, the resultant 3dB coupling length L_{π} will be shorter and as increase waveguide width (W) then increases 3dB coupling length exponentially. It is also observed that the coupling length for TM and TE unchanged, thus, MMI coupler could be realize fabrication tolerance and polarization insensitive device. From the table 3.2, smallest device can be realised in silicon, but it has sophisticated fabrication method and due

to very small device may have fabrication tolerance. Amongst these material, SU-8 polymer MMI coupler has shortest 3dB coupling length, it could be promising material of optical structure for optical communication system consideration. 3dB coupling length for *TE* and *TM* mode are approximately same with particular simulating material. it means MMI coupler can be demonstrated polarization insensitive device and fabrication tolerance as well. This study shows, MMI coupler can be also design and optimize as grating assisted coupler for wavelength Multiplexing/Demultiplexing within optical communication.

REFERENCES

- [1] Hunsperger, R. G., ed. [1991], Theory of Optical Waveguides, 3rdedition, Springer.
- [2] Yap, K. P., Delage, A., Lapointe, J., Lamontagne, B., Schmid, J. H., Waldron, P., Syrett, B. A. and Janz, S. [2009], 'Correlation of scattering loss, sidewall roughness and waveguide width in silicon-on-insulator (soi) ridge waveguides', Journal of Lightwave Technology 27(18), 3999-4008.
- [3] Bogaerts, W. [2011], 'Compact single-mode silicon hybrid rib/strip waveguide with adiabaticbends', IEEE Photonics Journal 3(3), 422-32.
- [4] Kaminow, I. P. [2008], 'Optical integrated circuits: a personal perspective', Journal of Light wave Technology 26(9), 994-1004.
- [5] Park, H., Sysak, M. N., Chen, H. W., Fang, A. W., Liang, D., Liao, L., Koch, B. R., Bovington, J., Tang, Y. and Wong, K. [2011], 'Device and integration technology for silicon photonic transmitters', Selected Topics in Quantum Electronics 17(3), 671-688.
- [6] Orcutt, J. S., Moss, B., Sun, C., Leu, J., Georgas, M., Shainline, J., Zraggen, E., Li, H., Sun, J. and Weaver, M. [2012], 'Open foundry platform for high-performance electronic photonic integration', Optics express 20(11), 222-232.
- [7] Tsao, S. and Chu-yi, L. [2002], 'BMP Simulation and comparison of 1x2 Directional waveguide coupling and Y-Junction coupling Silicon-on-Insulator optical coupler', Fiber and Integrated Optics 21, 417-433.
- [8] Zhang, Y., Yang, S., Lim, A. E., Lo, G. Q., Galland, C., Baehr-Jones, T. and Hocheber, M. [2013], 'A compact and low loss Y-junction for submicron silicon waveguide', Optics Express 21(1), 1310-1316.
- [9] Yamada, A. H., Chu, T., Ishida, S. and Arakawa, Y. [2005], 'Optical directional coupler based on si-wire waveguides', IEEE Photonics Technology Letters 17(3), 585-587.
- [10] Sheng, Z., Wang, Z., Qiu, C., Li, L., Pang, A., Wau, A., Wang, X., Zou, S. and Gang, F. [2012], 'A compact and low loss MMI coupler fabricated with CMOS technology', IEEE Photonics Journal 4(6), 2272-2277.
- [11] Chen, M., Liu, Z., Rong, L., Yang, Y., Lianh, M. and Tian-tong, T. [2013], 'An ultra compact optical directional coupler based on lithium niobate photonic wire', Optik 124, 1974-1976.
- [12] Stevanus, D. and Chee-Wei, L. [2005], 'A Rigorous Comparative Analysis of Directional Coupler and Multimode Interferometers Based on Ridge waveguides', Selected topics in Quantum electronics 11(2), 466-475.
- [13] COMSOL [2015], <http://www.comsol.com>.
- [14] Beam Pro [2014], <http://www.rsoftdesign.com>.
- [15] Jun-long, K., Xu, F. and Yan-qing, L. [2012], 'Loop-mirror-based slot waveguide refractive index sensor', Journal of Applied Physics Advances 2, 0421426.
- [16] Ofusa, N., Saito, T., Shimoda, T., HanaDa, T., Urino, Y. and Kitamura, M. [1999], 'An optical add-drop multiplexer with grating-loaded directional coupler in silica waveguide', IEIECE Trans. Commun. E82-B, 1248-1251.
- [17] Kogelnik, H. and Schmidt, R. V. [1976], 'Switched directional coupler with alternating', IEEE Journal of Quantum Electronics 12(7), 396-401.
- [18] Ternoven, R. Y., Honkamen, S. and Naja, S. I. [1993], 'Analysis of Symmetrical Directional coupler and Asymmetric Mach-Zehnder Interferometer as 1.3 μm and 1.5 μm Dual Wavelength Demultiplexer/Multiplexer', Journal Non-Linear Optic and Materials pp. 201-2065.
- [19] Lui, M. J. [2005], Photonic Device, Cambridge University Press.
- [20] Yamada, A. H., Chu, T., Ishida, S. and Arakawa, Y. [2005], 'Optical directional coupler based on si-wire waveguides', IEEE Photonics Technology Letters 17(3), 585-587.
- [21] Reed, G. and Knights, A. P. [2005], Silicon Photonics, John Wiley & Sons.

- [22] Il'ichev, I. V., Kozlov, A. S., Gaenko, P. V. and Shamray, A. V. [2009], 'Optimisation of the proton-exchange technology for fabricating channel waveguides in Niobate crystals', *Quantum Electronics* 39(1), 98-104.
- [23] Hongsik, J. [2016], 'Ti:LiNbO₃ integrated optic electric-field sensors based on electro-optic effect', *Fiber and Integrated Optics* 35(4), 161-180.
- [24] Chollet F, Liu H. B, M Ashraf, B Thubthimthong, X M Zhang, G Hegde, A Asundi, V M Murukeshan and A Q Liu, 'Of light, of MEMS: Optical MEMS in telecommunications and beyond,' *Sadhana* Vol. 34, Part 4, August 2009, pp. 599–606. © Printed in India
- [25] Wayant, R. W., ed. [2000], *Electro-optic hand book*, 2nd edition, Mc-Graw hill.
- [26] Nordstrom, M., Zauner, D. A., Boisen, A. and Hubner, J. [2007], 'Single Mode Waveguide with SU-8 Polymer core and cladding for MOEMS application', *Journal of Lightwave technology* 25(5), 1284-1289.
- [27] Gharffari, Moni, F., Djavid, M. and Abrishamian, M. S. [2008], 'Analysis of photonics crystal power splitters with different configurations', *Journal of Applied Sciences* 8(8), 1416-1425.
- [28] Xiea, S. Q., Wana, J., BingRui, L., Sunb, Y., Chenc, Y., XinPing, Q. and Ran, L. [2008], 'A nano-imprints lithography for fabrication of SU-8 gratings for near-infrared to deep UV applications', *Microelectronic Engineering* 85(5-6), 914-917.
- [29] Soldano, L. B. and Penning, E. C. M. [1995], 'Optical Multi-Mode Interference Devices Based on Self-Imaging; Principles and Applications', *Journal of Lightwave Technology* 13(4), 615-627.